Periodica Polytechnica
Civil Engineering

60(4), pp. 661–667, 2016
DOI: 10.3311/PPci.8763

RESEARCH ARTICLE

Rheological-Dynamical Continuum Damage Model Applied to Research of the Rotational Capacity of a Reinforced Concrete Beams

Dragan D. Milašinović, *Danica* Goleš, *Arpad* Čeh
Received 05-11-2015, accepted 15-02-2016

Abstract

In this paper a new rheological-dynamical continuum damage model for concrete under compression is used to research the behaviour of reinforced concrete beams subjected to bending. Within the framework of this approach the stress-strain curve of a concrete under compression in the pre-peak regime can be computed if the compressive strength, elastic modulus, concrete density and Poisson's ratio are experimentally evaluated. The ultimate strain is determined in the post-peak regime only, using the secant stress-strain relation from damage mechanics. Experimental stress-strain data in the pre-peak regime for five concrete compositions were obtained during the examination presented herein. The numerical predictions regarding moment-curvature and ductility of a reinforced concrete beam are presented for five concrete compositions, demonstrating capabilities of a new analytical model.

Keywords

concrete under compression · stress-strain curve · reinforced concrete beam · rotational capacity

Dragan D. Milašinović
Faculty of Civil Engineering, University of Novi Sad, Subotica, Kozaračka 2a, Serbia
e-mail: ddmil@gf.uns.ac.rs

Danica Goleš
Faculty of Civil Engineering, University of Novi Sad, Subotica, Kozaračka 2a, Serbia
e-mail: dgoles@gf.uns.ac.rs

Arpad Čeh
Faculty of Civil Engineering, University of Novi Sad, Subotica, Kozaračka 2a, Serbia
e-mail: ceh@gf.uns.ac.rs

1 Introduction

Reinforced concrete materials have been studied and employed in diverse fields of science and engineering disciplines due to their wide application in infrastructure in many countries. From a practical standpoint, the ultimate strength design of reinforced concrete elements brought the stress-strain curve into focus. The stress-strain curve of concrete under compression, and in particular the compressive strength, ultimate strain and post-peak branch, have an important role in the design of concrete and concrete-based structures.

In the last three decades, there has been a keen interest in compressive failure. In the early 1990's, an extensive Round/Robin test on compressive softening was carried out by the RILEM Technical Committee 148-SSC [1]. Compression failure can have a great variety of forms both from theoretical and experimental viewpoints, while the mode of failure is complex. The principal difference from tensile fracture is that there is a residual stress in the specimens. The correct evaluation of the constitutive parameters is also complicated by many other testing aspects. To interpret the test results, it is important to know the influence of the boundary conditions on the slope of the load-displacement curve and on the value of the crushing energy [2]. An in-depth review of this matter as well evidence that slenderness of the specimen has influence on the collapse mechanism is given in [3]. Considering the size-scale and slenderness effects in uniaxial compression tests, Carpinteri et al. [4] proposed an analytical model based on the concept of strain localization.

Ductile and durable concrete structures are the goal of all designers. In order to achieve such goals it is necessary to know the laws that govern the behavior of materials and structures for both nonlinearities: the geometrically nonlinear effects [5] and nonlinear behaviour of the material caused by an inelastic deformation. Analytical models of time-dependent stress-strain response of concrete under compression are required. For global failure analysis, the failure mechanism must be treated in a smeared manner, as a continuum with damage. Since about 1998 (Milašinović, [6, 7]), a mathematical-physical analogy named rheological-dynamic analogy (RDA) has been pro-

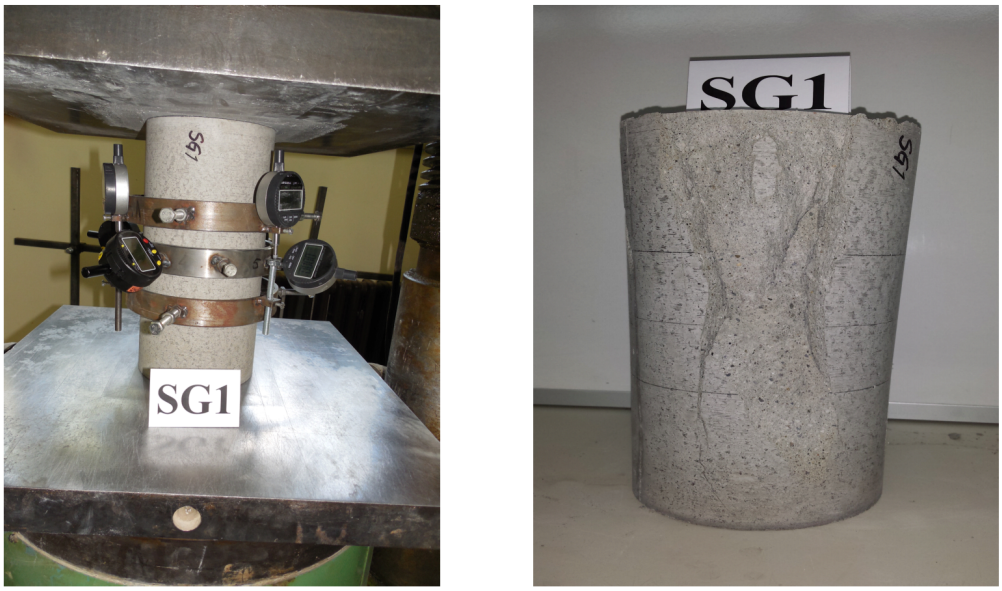

Fig. 1. Tested cylinder SG1 before (left) and after encumbering (right)

posed in explicit form to predict a range of inelastic and time-dependent problems related to 1D prismatic rods, such as buckling, fatigue etc. This theory defines the critical mechanical properties of viscoelastoplastic (VEP) materials. RDA is based on the propagation of elastic waves under instantaneously applied impact loading. A successful theoretical approach based on RDA and their practical applications have also been given in connection with the VEP behavior of metallic bars in tension [8]. In fact, cracking is accompanied by an emission of elastic waves which propagate within the bulk of the material. Continuum damage mechanics is a mechanical theory for analyzing damage and fracture processes in materials from a continuum mechanics point of view including different scales of the damage observation [9].

The aim of this paper is to apply rheological-dynamical continuum damage model to research of the rotational capacity of a reinforced concrete beams. Many researchers have tried to represent the stress-strain relationship with standard mathematical curves, e.g., a parabola, hyperbola, ellipse, cubic parabola, or combinations like a parabola with a straight line and so on, see also *fib* Model Code for Concrete Structures 2010 [10]. These curves may have the advantage of simplifying the computation of the ultimate moment of reinforced concrete sections. However, they can be classified only as empirical methods since the assumed stress distribution does not represent an observed physical phenomenon, such as the failure mechanism. Moreover, to identify global failure as a continuum with damage, the damage variable must be formulated first. The proposed stress-strain curve given by the first author in [11] is shown to provide very good predictions for the stress versus strain response in the pre-peak regime. Within this global model the three main failure characteristics, the residual stress, the critical value of interpenetration displacement and the crushing energy, are theoretically evaluated. Finally, on the basis of four non-dimensional constants the crushing energy is calculated for five concrete compositions. Using the proposed model, the theoretical relations between bending moment and the curvature of a reinforced concrete beam, for expressing the ductility in bending through the rotational capacity, are presented in this paper.

2 Comparative analysis for five concrete compositions

2.1 Average RDA stress-strain curve

The RDA modulus function has been used in [11] to obtain the quasi-static stress-strain curve, as follows

$$\varepsilon = \frac{\sigma_{cr}}{E_R(0)} = \frac{\sigma_{cr}}{E(0)}(1+\varphi_{cr}) = \frac{\sigma_{cr}}{E(0)}(1+\sigma_{cr}K_E) \qquad (1)$$

Thus, one quadratic equation takes the form of

$$\sigma_{cr}^2 K_E + \sigma_{cr} - E(0)\,\varepsilon = 0 \qquad (2)$$

Slope $E(0)$ is the elastic modulus of the material in its initial state. The root of Eq. (2) under the initial conditions $\varepsilon(0)=0$ and $\sigma_{cr}(0)=0$ is the limit value of critical stress for the selected strain or the average stress-strain curve. Then

$$\sigma_{cr} = \frac{1}{2K_E}\left(\sqrt{1+4K_E E(0)\,\varepsilon}-1\right). \qquad (3)$$

At the limit of elasticity, the slope is equal to the elastic modulus E_H (known value). Therefore,

$$E_R(0) = E_H. \qquad (4)$$

Thus,

$$E(0) = E_H(1+\varphi^*). \qquad (5)$$

Tab. 1. Experimentally evaluated mechanical properties for five concrete compositions

Type of concrete	Concrete density [kg/m^3]	Elastic modulus E_H [MPa]	Poisson's ratio	Compressive strength f_c [MPa]
HCS-04	2289	49211	0.175	76.82
SG1	2265.5	30994	0.185	65.91
NSC	2325	28700	0.217	57.27
CC-1	2228.6	27404	0.180	38.90
C20	2125	23421	0.165	25.00

HCS-04 Repair mortar cement, polymers, minerals, and chemicals and fillers-based;
SG1 SikaGrout 212 repair mortar;
NSC Normal-strength concrete;
CC-1 Normal-strength concrete;
C20 Concrete strength class

Tab. 2. Numerically defined dynamic and static RDA curves for five concrete compositions

	Dynamic RDA curve	Static RDA curve
HCS-04	$\frac{1}{2\cdot 0.017054}\left(\sqrt{1+4\cdot 0.017054\cdot 75709.23\cdot\varepsilon}-1\right)$	$\frac{1}{2\cdot 0.032009}\left(\sqrt{1+4\cdot 0.032009\cdot 75709.23\cdot\varepsilon}-1\right)$
SG1	$\frac{1}{2\cdot 0.025344}\left(\sqrt{1+4\cdot 0.025344\cdot 49196.83\cdot\varepsilon}-1\right)$	$\frac{1}{2\cdot 0.047569}\left(\sqrt{1+4\cdot 0.047569\cdot 49196.83\cdot\varepsilon}-1\right)$
NSC	$\frac{1}{2\cdot 0.019906}\left(\sqrt{1+4\cdot 0.019906\cdot 50707.16\cdot\varepsilon}-1\right)$	$\frac{1}{2\cdot 0.037360}\left(\sqrt{1+4\cdot 0.037360\cdot 50707.16\cdot\varepsilon}-1\right)$
CC-1	$\frac{1}{2\cdot 0.030928}\left(\sqrt{1+4\cdot 0.030928\cdot 42818.75\cdot\varepsilon}-1\right)$	$\frac{1}{2\cdot 0.058048}\left(\sqrt{1+4\cdot 0.058048\cdot 42818.75\cdot\varepsilon}-1\right)$
C20	$\frac{1}{2\cdot 0.045456}\left(\sqrt{1+4\cdot 0.045456\cdot 34956.72\cdot\varepsilon}-1\right)$	$\frac{1}{2\cdot 0.085316}\left(\sqrt{1+4\cdot 0.085316\cdot 34956.72\cdot\varepsilon}-1\right)$

where φ^* is the structural creep coefficient and K_E is the structural-material constant at the limit of elasticity as detailed in [11].

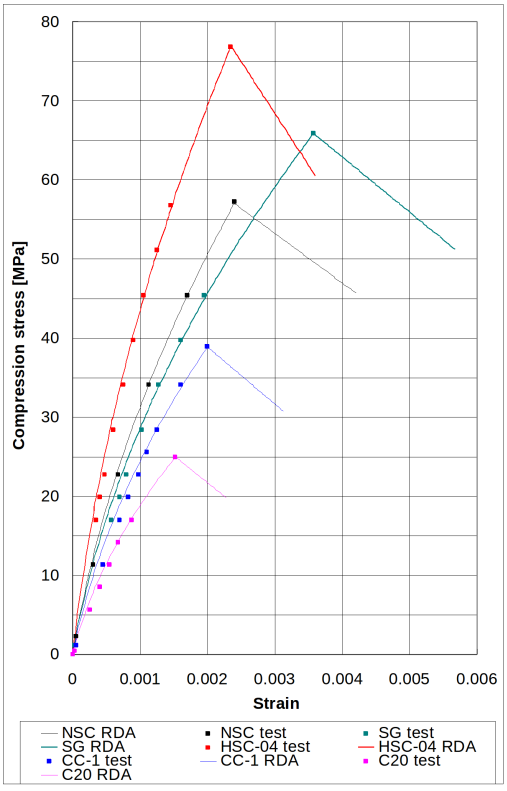

Fig. 2. Comparison of test data for stress-strain pairs and dynamic RDA curves for five concrete compositions

As detailed by Van Mier et al. [1], the stress-strain curves of concrete are dependent on two major groups of parameters: testing conditions and concrete characteristics. The key experimental parameters cited in [1] included the frictional restraint between the loading platen and the specimen, the rotation of the loading platen during the experiment, the gauge length of the control LVDT, the stiffness of the testing machine, the type of the feed-back signal, the loading rate, the shape and size of the test specimen and the concrete composition. It is therefore important when using experimental data for verification and comparison that the experimental parameters are fully listed. Concrete characteristics depend on many interrelated variables such as the water-cement ratio, the mechanical and physical properties of the cement and aggregate, and the age of the specimen when tested [12].

In this study, cylinders of slenderness $l_0/\Phi = 2$, loaded between the steel plates with low-friction are tested only (see Fig. 1).

The analytical stress-strain curve of concrete in the ascending branch is obtained as a critical curve and can be computed using Eq. (3) if the compressive strength, elastic modulus, concrete density and Poisson's ratio are experimentally evaluated. It is valid for various prismatic concrete samples (e.g., with a square or circular cross section A_0) and different concrete compositions.

To identify the basic mechanism that leads to concrete damage growth, some primary features of experimentally observed concrete behavior are presented first, see [11].

2.2 Experimental tests and model verifications

An experimental investigation was carried out to explain the compression behavior of standard concrete cylinders with a strength range of 20 - 80 MPa. The presented experimental research was conducted at the Materials and Structures Testing Laboratory of the Faculty of Civil Engineering in Subotica, Serbia. A series of tests were performed on five concrete composi-

Tab. 3. Main concrete properties and crushing energies calculated with four non-dimensional constants valid for all concrete compositions

Type of concrete	f_c [N/mm^2]	E_H [N/mm^2]	ε_{cr}	ε_{crF}	G_C [N/mm]
HCS-04	76.82	49211	0.00235	0.00361	**30.84**
SG1	65.91	30994	0.003577	0.00568	**41.32**
NSC	57.27	28700	0.0024	0.00427	**32.48**
CC-1	38.90	27404	0.002	0.00313	**14.08**
C20	25.00	23421	0.001525	0.00228	**6.33**

Fig. 3. Mode of failure of cylinder SG1 (left), and measured value of critical crack depth (right)

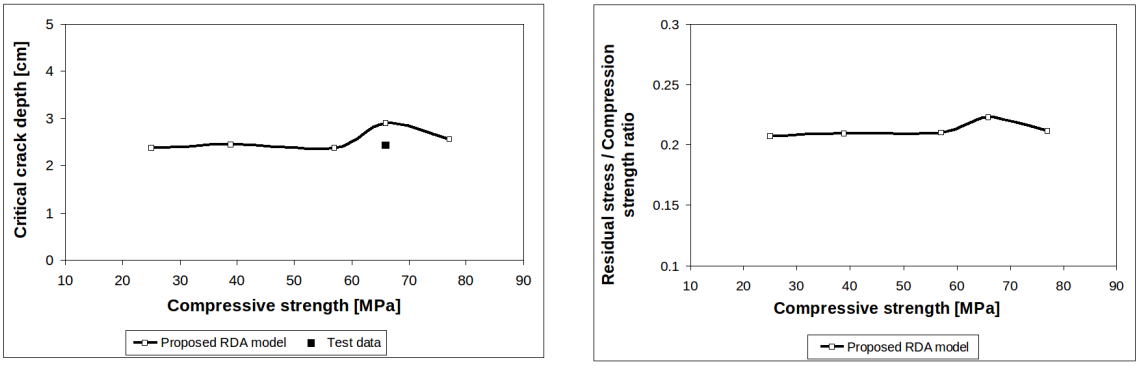

Fig. 4. Variation of critical crack depth and strength (left), and $\sigma_{residual}$ / σ_{crF} ratio and strength (right)

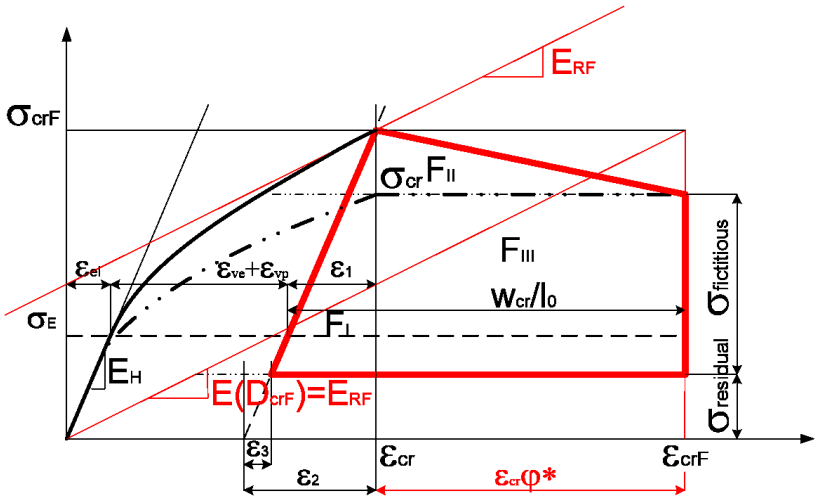

Fig. 5. Prediction of dynamic RDA stress-strain curve, dynamic strength $f_c = \sigma_{crF}$, ultimate strain ε_{crF} end crushing energy G_C [11].

tions. The measured values of concrete density, elastic modulus, Poisson's ratio and compressive strength are listed in Table 1.

The HCS-04 cylinder was made of a high-quality, two-component concrete mix, commercially available by the name PolimagHK-04. The liquid component contains water, cement polymer and plasticizer, while the powder component contains cement, crushed carbonaceous stone aggregates, powdered filler and minerals. These components were mixed in a concrete mixer and no additional materials were added. The SG type concrete was a high strength, low shrinkage, expanding material commercially known as SikaGrout212. It is a powdered concrete mix which contains cement, crushed stone aggregate and powdered cement additives. In accordance to the manufacturer recommendations, fresh concrete was prepared by adding 3.7 liters of drinking water to one 28 kg bag of SikaGrout. The mix proportions for other concrete compositions were: NSC (portland cement (PC) CEM II/B-M: 500 kg/m^3; water: 200 kg/m^3; fine aggregate: 991 kg/m^3; coarse aggregate: 633 kg/m^3), CC-1 (PC CEM II/A-M: 445 kg/m^3; water: 250 kg/m^3; fine aggregate: 465 kg/m^3; coarse aggregate: 1100 kg/m^3) and C20 (PC CEM II/B-M: 395 kg/m^3; water: 280 kg/m^3; sand: 420 kg/m^3; coarse aggregate: 1165 kg/m^3). The concrete mix was designed for compressive cylinder strength f_c at 28 days of approximately 20 - 80 MPa.

The numerically defined dynamic and static RDA curves are presented in Table 2. The acceleration coefficient $f_\gamma = 1.37$ was used in the computation for all concrete compositions as detailed in [11].

The experimentally evaluated and numerically computed dynamic stress-strain curves shown in Fig. 2 are in excellent agreement beyond the limit of elasticity, because the limit of elasticity is the border from which the rheological-dynamical theory is developed.

The failure mode of the standard concrete cylinder is also discussed in [11]. The relevant measured global property is critical crack depth shown in Fig. 3 left. As it is presented in Fig. 3 right and Fig. 4 left, the calculated values of critical crack depths are in excellent agreement with the measured value (2.43 cm).

According to the investigation detailed in [11], the critical interpenetration displacement w corresponds to

$\sigma_{residual} = 0.2124\,\sigma_{crF}$, see Fig. 4 right.

The theory presented in [11] describes the critical stress-strain response of material in compression before the peak for five different concrete compositions, which are experimentally verified. This approach covers also the degradation of stiffness and strength with limited ductility in the post-peak regime, because it combines damage mechanics. The area below the stress-strain curve shown in Fig. 5 represents the crushing energy per unit area for standard concrete cylinders, which can be calculated from ($f_c = \sigma_{crF}$, E_H [MPa])

$$G_C = 93 \cdot \frac{f_c^2}{E_H} + 204 \cdot f_c \cdot (\varepsilon_{crF} - \varepsilon_{cr}), \tag{6}$$

with four non-dimensional constants valid for all concrete compositions

$$\begin{aligned} &\sigma_{residual}/f_c = 0.2124,\\ &\sigma_S/f_c = 0.7876,\\ &a/g = f_c/\sigma_S - 1 = 0.27,\\ &f_\gamma = \frac{1}{1-a/g} = 1.37. \end{aligned} \tag{7}$$

The residual stress level is what principally distinguishes compression fracture from tensile fracture, but it is a consequence of the uniformly accelerated motion of load during the examination of compressive strength.

The main concrete properties which must be used for the numerical calculation of the crushing energy by Eq. (6) are given in Table 3.

3 Behaviour of reinforced concrete beam in bending

All limit design theories are based on the principals of equilibrium of internal forces and compatibility of deformations at the state of impending failure, see Fig. 6 left.

The here presented model for the analysis of the behaviour of reinforced concrete beam in bending is based on the assumptions that plane cross-sections remain plane and that the behaviour of concrete in compression is in compliance to the dynamic RDA stress-strain curve. The stress-strain curve of reinforcement is assumed as bilinear elastic-perfectly plastic, Fig. 6 right. The influence of reinforcement in compression and the effect of confinement due to stirrups are not considered here. The contribution of the cracked concrete in tension is neglected. Hence, the dimensionless moment-curvature relations and ductility of reinforced concrete beams are analyzed by means of a new approach, where the dynamic RDA curves for five concrete compositions are taken into account. This leads to a strong dependency of the ductility from the four experimentally evaluated properties of the concrete (concrete density, elastic modulus, Poisson's ratio and compressive strength).

According to Fig. 6 left, the strain ε_0 at the peak stress σ_{cr} and the ultimate strain ε_u of concrete in compression may be expressed as follows

$$\begin{aligned} \varepsilon_0 &= \frac{\sigma_{crF} - \sigma_{residual}}{E_H} = \frac{\sigma_{cr}}{E_H} = \varepsilon_2 - \varepsilon_3\\ \varepsilon_u &= \varepsilon_{crF} - \varepsilon_{cr} + \frac{\sigma_{cr}}{E_H}. \end{aligned} \tag{8}$$

From similitude of triangles in Fig. 6 left the strain of the reinforcement may be obtained as

$$\varepsilon_s = \frac{1-\xi}{\eta}\varepsilon_0 = \frac{1-\xi}{\eta}\frac{\sigma_{cr}}{E_H} \tag{9}$$

In Fig. 6 left, $x = \xi d$ is the depth of the compression zone, and d is the effective depth of the beam. In the post-peak regime,

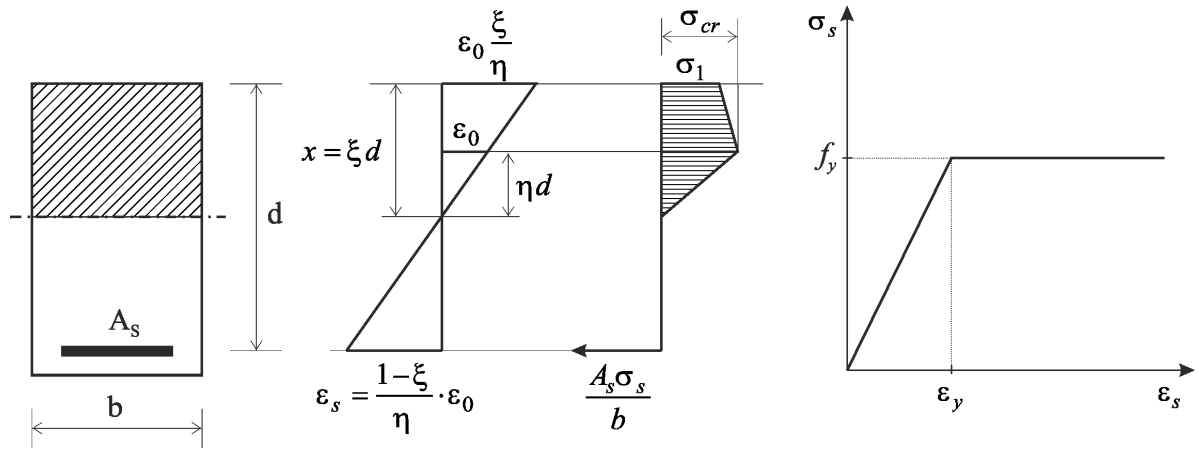

Fig. 6. Strain and stress distribution in a rectangular cross-section (left), and bilinear stress-strain curve for reinforcement (right)

where $\sigma_{fictitious} \leq \sigma_1 \leq \sigma_{cr}$, the stress ratio σ_1 / σ_{cr}, is given by

$$\frac{\sigma_1}{\sigma_{cr}} = \frac{\varepsilon_{crF} - \varepsilon_{cr} + \frac{\sigma_{crF} - \sigma_{cr}}{E_H}\left(1 - \frac{\xi}{\eta}\right)}{\varepsilon_{crF} - \varepsilon_{cr}} \tag{10}$$

The condition of force equilibrium gives

$$\frac{A_s \sigma_s}{bd\sigma_{cr}} = \frac{1}{2}\left(\xi + \frac{\sigma_1}{\sigma_{cr}}(\xi - \eta)\right) \tag{11}$$

where A_s and σ_s are the cross sectional area and tensile stress of reinforcement, respectively. Also, the dimensionless bending moment may be expressed as follows

$$\frac{6M}{bd^2\sigma_{cr}} = \xi(3 - 2\xi + \eta) + \frac{\sigma_1}{\sigma_{cr}}(\xi - \eta)(3 - \xi + \eta) \tag{12}$$

The curvature κ can be obtained as

$$\kappa = \frac{1}{r} = \frac{\varepsilon_0}{\eta d} = \frac{\sigma_{cr}}{E_H \eta d} = \frac{\varepsilon_2 - \varepsilon_3}{\eta d}. \tag{13}$$

According to Eqs. (8) to (13), the dimensionless bending moment-curvature relations of reinforced concrete beams are obtained for five concrete compositions described in Section 2.2 (Table 1, Table 2 and Table 3) and shown in Fig. 7 to Fig. 10, for reinforcement ratios $A_s / bd =$ 0.02, 0.03, 0.04 and 0.05. Adopted properties of the reinforcing steel are: $f_y = 400$ MPa and $E_s = 200000$ MPa. As expected, the beams made of concrete with higher compressive strength have more ductile behaviour, even with higher reinforcement content (e.g. HCS-04, SG1). On the other hand, if the concrete with low compressive strength is used, a brittle behaviour occurs even at low reinforcement ratios (e.g. C20). Hence, it is obvious that an optimization approach to find the best concrete composition may be useful.

The ductility in bending is here expressed as the ratio between the ultimate curvature κ_u and the curvature κ_{sy}, which corresponds to the condition of reaching the yield strength of reinforcement. The relation between ductility and reinforcement ratios for five concrete compressive strengths is shown in Fig. 11.

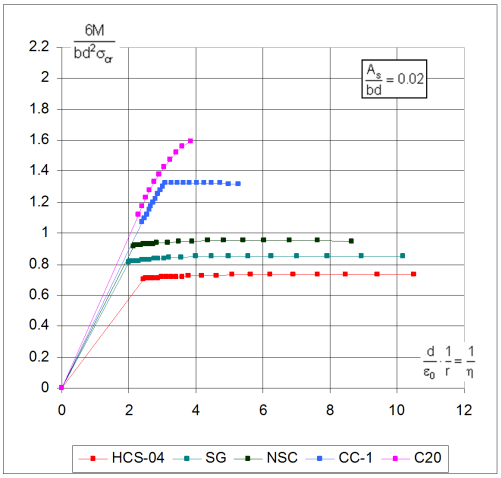

Fig. 7. Dimensionless bending moment-curvature relations for reinforcement ratio 0.02

In the case of the SG1 concrete the most favorable failure characteristics are obtained if the criterion of the ductility in bending is adopted as authoritative.

4 Conclusions

The approach proposed in [11] for global failure analysis of concrete in compression combines the RDA and damage mechanics. The present study analyzes experimentally five different concrete compositions. Finally, the test results are used for the analysis of moment-curvature and compressive strength-reinforcement ratio-ductility relations of reinforced concrete beam in bending. The results of this paper also indicate the possible direction of further studies in the field of reinforced-concrete structures. It is important to emphasize that the measured concrete properties are characterized by much higher dispersion than the relevant parameters which characterize the failure mode of concrete cylinders. Hence, it is obvious that an optimization approach to find the best concrete mixture may be useful.

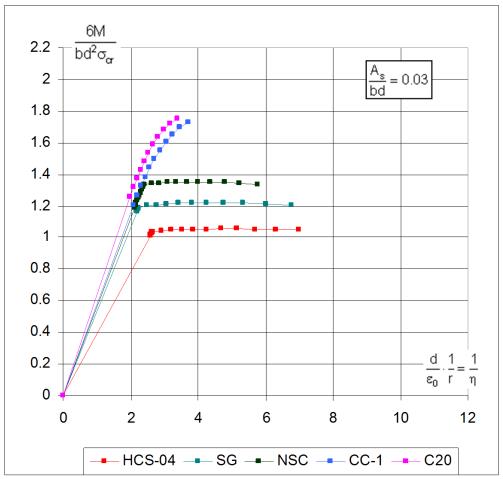

Fig. 8. Dimensionless bending moment-curvature relations for reinforcement ratio 0.03

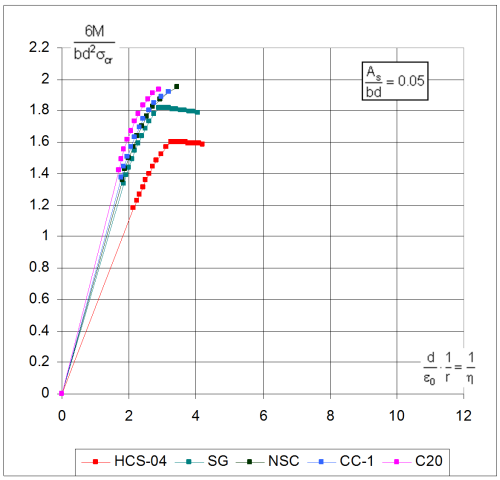

Fig. 10. Dimensionless bending moment-curvature relations for reinforcement ratio 0.05

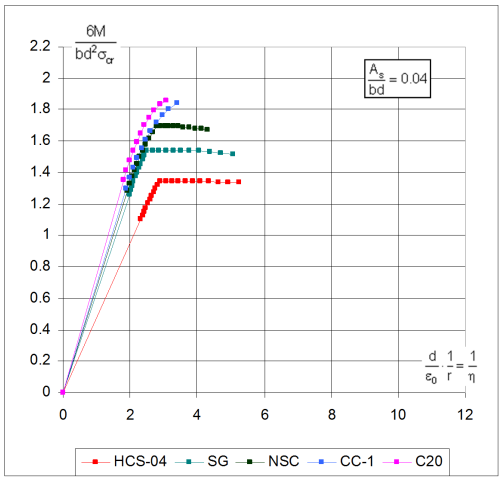

Fig. 9. Dimensionless bending moment-curvature relations for reinforcement ratio 0.04

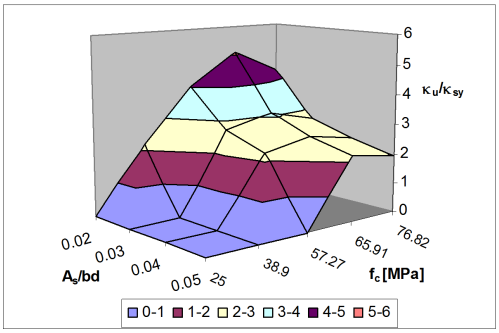

Fig. 11. Ductility-reinforcement ratio relation for five concrete compressive strengths

Acknowledgement

The work presented in this paper is a part of the investigation conducted within the research projects ON 174027 "Computational Mechanics in Structural Engineering" and TR 36017 "Utilization of by-products and recycled waste materials in concrete composites for sustainable construction development in Serbia: investigation and environmental assessment of possible applications", supported by the Ministry of Science and Technology, Republic of Serbia. This support is gratefully acknowledged.

References

1 **Van Mier JGM, Shah SP, Arnaud M, Balayssac JP, Bascoul A, Choi S, Dasenbrock D, Ferrara G, French C, Gobbi ME, Karihaloo BL, Konig G, Kotsovos MD, Labuz J, Lange-Kornbak D, Markeset G, Pavlovic MN, Simsch G, Thienel K-C, Turatsinze A, Ulmer M, van Geel HJGM, van Vliet MRA, Zissopoulos D**, *Strain-softening of concrete in uniaxial compression*, Materials and Structures, **30**(4), (1997), 195–209, DOI 10.1007/BF02486177.

2 **Kotsovos MD**, *Effect of testing techniques on the post-ultimate behaviuor of concrete in compression*, Materiaux et Constructions, **16**(91), (1983), 3–12, DOI 10.1007/BF02474861.

3 **Indelicato F, Paggi M**, *Specimen shape and the problem of contact in the assessment of concrete compressive strength*, Materials and Structures, **41**(2), (2008), 431–441, DOI 10.1617/s11527-007-9256-7.

4 **Carpinteri A, Corrado M, Paggi M**, *An Analytical Model Based on Strain Localisation for the Study of Size-Scale and Slenderness Effects in Uniaxial Compression Tests*, Strain, **47**, (2011), 351–362, DOI 10.1111/j.1475-1305.2009.00715.x.

5 **Milasinovic DD, Goles D**, *Geometric Nonlinear Analysis of Reinforced Concrete Folded Plate Structures by the Harmonic Coupled Finite Strip Method*, Periodica Polytechnica Civil Engineering, **58**(3), (2014), 173–185, DOI 10.3311/PPci.2096.

6 **Milasinovic DD**, *Rheological-dynamical analogy: prediction of buckling curves of columns*, International Journal of Solids and Structures, **37**(29), (2000), 3965–4004, DOI 10.1016/S0020-7683(99)00211-5.

7 **Milasinovic DD**, *Rheological-dynamical analogy: modeling of fatigue bahavior*, International Journal of Solids and Structures, **40**(1), (2003), 181–217, DOI 10.1016/S0020-7683(02)00518-8.

8 **Milasinovic DD**, *Rheological-dynamical analogy: visco-elasto-plastic behaviour of metallic bars*, International Journal of Solids and Structures, **41**(16-17), (2004), 4599–4634, DOI 10.1016/j.ijsolstr.2004.02.061.

9 **Murakami S**, *Continuum Damage Mechanics*, Springer; Netherlands, 2012.

10 *Fib Model Code for Concrete Structures 2010*, Wilhelm Ernst & Sohn; Berlin, 2013.

11 **Milasinovic DD**, *Rheological-dynamical continuum damage model for concrete under uniaxial compression and its experimental verification*, Theoretical and Applied Mechanics, **42**(2), (2015), 73–110, DOI 10.2298/TAM1502073M.

12 **Chen X, Wu S, Zhou J**, *Experimental study and analytical formulation of mechanical behavior of concrete*, Construction and Buildings Materials, **47**, (2013), 662–670, DOI 10.1016/j.conbuildmat.2013.05.041.